A Heat Exchanger Reactor Equipped with Membranes to Produce Dimethyl Ether from Syngas and Methyl Formate and Hydrogen from Methanol

A. Bakhtyari, A. Darvishi, and M.R. Rahimpour*

Department of Chemical Engineering, School of Chemical and Petroleum Engineering, Shiraz University, Shiraz 71345, Iran

Abstract: The energy crisis of the century is a motivation to present processes with higher energy efficiency for production of clean and renewable resources of energy. Hence, a catalytic heat exchanger reactor for production of dimethyl ether (DME) from syngas, and hydrogen and methyl formate (MF) from methanol is investigated in the present study. The proposed configuration is equipped with two different membranes for in-situ separation of products. Syngas is converted to DME through an exothermic reaction and it supplies a part of required energy for the methanol dehydrogenation reaction. Produced water in the exothermic side and produced hydrogen in the endothermic side are separated by using appropriate perm-selective membranes. In-situ separation of products makes the equilibrium reactions proceed toward higher conversion of reactants. A mathematical model based on reasonable assumptions is developed to evaluate molar and thermal behavior of the configuration. Performance of the system is aimed to enhance by obtaining optimum operating conditions. In this regard, Genetic Algorithm is applied. Performance of the heat exchanger double membrane reactor working under optimum conditions (OTMHR) is compared with a heat exchanger reactor without membrane (THR). OTMHR promotes methanol conversion to MF to %87.2, carbon monoxide conversion to %95.8 and hydrogen conversion to %64.6.

Keywords: Energy resources, Thermally-coupled reactors, Membrane reactors, Genetic algorithm.

1. INTRODUCTION

With respect to growing energy consumption in household and industrial sections, environmental issues and finite sources of hydrocarbons, investigating alternative sources of energy and protocols to solve energy problem is crucial. Followings are possible strategies for solving energy problem:

- Making the industries switch away from fossil fuels towards more efficient energy sources
- Developing in-situ energy production technologies such as on-board hydrogen production facilities
- Utilizing energy generation technologies using new sources of energy such as biomass, wind, solar, and geothermal power
- Developing onsite technologies with combined heat and power applications
- Retrofitting or replacing well-worn equipment

Chemical industries are considered as cornerstone in economy of governments. However they are one of the main users of energy sources such as natural gas, liquefied petroleum gas (LPG) and natural gas liquid (NGL) [1]. Hence, reformations in equipment configurations may result in reducing energy consumption in chemical industries. On the one hand, seeking for energy efficient processes with no decline in productivity of the process and quality of the products poses a challenge to chemical industries [2-4]. Process intensification (PI) as a modern design approach in chemical industries, is running the art of increasing productivity of the process and qualities of the products with lower energy and feed stocks consumption. Designing heat-integrated equipment using generated heat in one section to drive processes in other section is a task of PI. In fact, the produced heat in a part of system could be recovered and utilized for heating or running the endothermic processes in the other part. Such a standpoint is practical in designing chemical reactors due to existence of vast exothermic and endothermic reactions in chemical industries [5-7].

1.1. Heat Exchanger Reactors: A Novel Energy Saving Method by Thermally Coupling

Chemical reactors, the heart of chemical industries, play a significant role in PI.A vast variety of chemicals is produced through exothermic reactions with high heat generation rate. The generated heat could be recovered and used. Besides, many chemicals are produced with endothermic reactions (*e.g.*

*Address correspondence to this author at the Department of Chemical Engineering, School of Chemical and Petroleum Engineering, Shiraz University, Shiraz 71345, Iran; Tel: +98 711 2303071; Fax: +98 711 6287294; E-mail: rahimpor@shirazu.ac.ir

E-ISSN: 2410-1869/16

dehydrogenation) requiring a heat source to drive the reaction. The produced heat in the exothermic side could be transferred to the endothermic side with a heat exchanger reactor. For this purpose, two reactions are integrated in a shell and tube. Therefore, heat of exothermic reaction is captured and used to make the endothermic reaction start and proceed. As a result, thermal efficiency of the reactor is increased and less energy is consumed. That is why heat exchanger reactors are vast field of study and have attracted attentions of researchers and industries [8]. Rahimpour and colleagues have studied various exothermic and endothermic reactions in coupled or double coupled fixed bed and fluidized bed reactors. Application of this concept in diverse processes such as GTL technology and Fischer–Tropsch synthesis [9-12], naphtha reforming [13-16], syngas production, methanol synthesis and DME synthesis was investigated [17-27]. More information of thermally coupled reactors and their benefits and drawbacks are gathered in a review by Rahimpour *et al*. [8].

1.2. Membrane Reactors: Highly Energy Efficient Separations and Yield Enhancement

Both separation and chemical reaction are possible solely or simultaneously in a membrane reactor. Membrane characteristics, such as high surface area per unit volume, high selectivity and permeability and possibility of controlling permeation rate, make it promising for simultaneous reaction and separation [28, 29]. Besides, high efficient phase separations are achieved by using perm-selective membranes. Unlike the typical separation methods *e.g*. distillation (with 3% share in the worldwide energy consumption [30]), phase change is not essential in separation of mixture ingredients by using membranes. Therefore, thermal equipment such as rebolilers is omitted which is leading to noticeable energy saving. On the other hand, membrane reactors are promising to overcome disadvantages of traditional separation techniques. However, decline in high temperature and pressure reacting systems and clean up inconvenience narrow application of membranes. Yield/selectivity enhancement and thermodynamically shift the equilibrium reactions toward products are broadly investigated in systems with hydrogen and water recovery [31-34]. Application of hydrogen perm-selective membranes for hydrogen recovery from hydrocarbon processing units and in-situ hydrogen production and separations in dehydrogenation reactions is currently of a great interest [32].

1.3. Dimethyl Ether (DME): A Clean Energy Resource for Meeting Strict Emissions Standards

Fossil fuels with 80 % share in supplying worldwide energy requirement cause some environmental problems such as global warming, climate change and defects in biodiversity [35]. These issues make the researchers and concerned industries investigate clean sources of energy. Chemical and petrochemical industries as the largest energy consumers among industries are responsible for introducing green or less harmful alternatives for energy supply.

DME (which is also known as methoxymethane) is the isomer of ethanol and the simplest ether. It is a volatile, non-toxic, colorless and clean-burning gas. Ignition characteristics of DME are similar to those of butane and propane. Hence, it is classified as an LPG [36]. DME becomes liquid at pressures beyond 5 bar. Then, it is easily stored and transported without need to high-pressure containers. Simple engines with low maintenance charges, no need to spark plugs and efficient performance in ignition of compressed DME are benefits of engines working with DME. To meet strict standards of emissions, DME has following merits [37]:

- No C-C bonds leading to lower CO emission rather than natural gas
- No explosive peroxides leading to easy and safe transportation and storage
- High cetane number and no NO_x emission

Chemicals such asdimethyl sulfate, methyl acetate and lower olefins are produced directly or indirectly from DME. Besides, it is used as polishing agent and green refrigerant. Much attention of industries and researchers is attracted to DME due to the aforementioned virtues [38-43].

There are single-step and two-step routes to produce DME from syngas. In the single-step route, a hybrid catalyst for simultaneous methanol synthesis and dehydration is used [44-46]. While, in the two-step route, formerly synthesized methanol is dehydrated to DME [37, 38]. Simultaneous methanol production and conversion by hybrid catalyst can eliminate thermodynamic limitations of CO conversion to methanol. Besides, intermediate facilities for methanol purification (that are energy intensive) are eliminated [46-48]. In spite of primacy of the single-step route,

separation of unreacted syngas and CO_2 from the output stream is inconveniences of this route [49-50]. Accordingly, any enhancement in the conversion of syngas to higher purity of DME in the product stream is appreciated by linked industries.

1.4. Methyl Formate (MF): Next Candidate of C_1 Chemistry

C_1 chemistry concerns with producing valuable multi-carbon compounds from single-carbon compounds such as carbon dioxide, carbon monoxide, methanol and syngas. An introduced building block in C_1 chemistry must be produced in an efficient route. Besides, it must be efficiently converted to downstream products [51, 52]. MF (also known as methyl methanoate) is introduced as a promising building block in C_1 chemistry in the next future. Followings are merits of MF [51-56]:

- various routes to produce MF *e.g*. direct synthesis from syngas, dehydrogenation of methanol, oxidative dehydrogenation of methanol, dimerization of formaldehyde, hydro condensation of carbon dioxide with methanol and carbonylation of methanol
- Molecule with one more CO than that of methanol raising it as a promising CO/H_2 mixture
- Convertible to formic acid, form amide and dimethylformamide
- Storing, handling and transporting almost the same as LPG

MF is a colorless and toxic compound with ethereal smell. At moderate pressures and temperatures, it is in liquid state with high vapor pressure (normal boiling point is 31.5 °c). MF is industrially produced by BASF technology with 96% selectivity of methyl formate [57]. Proposing novel energy efficient routes to manufacture MF is currently state of the art.

1.5. Hydrogen: The Only Non-Pollutant Element for Energy Delivery

As previously mentioned, environmental problems of burning fossil fuels such as global warming, emission of toxic pollutants *e.g.* NO_x, SO_x, climate change, defects in biodiversity and even limited sources of fossil fuels are motivations of researchers and industries toward exploring new clean, renewable and sustainable energy alternatives [58, 59]. Although hydrogen is an energy carrier, not an energy source, it may be considered as a good candidate for energy delivery. Beneficial characteristics *e.g*. environmentally friendly nature and efficient ignition are reasons of increasing demand for hydrogen. Besides, hydrogen is a promising choice for energy alteration due to the following advantages [60, 61]:

- High heating value comparing fossil fuels
- Non-pollutant and non-toxic emissions
- Raw material in various chemical and petrochemical industries
- Fuel for vehicle engines and power plants
- Renewability and sustainability

Hydrogen is commercially produced by steam or dry reforming of hydrocarbons, coal and biomass gasification, partial oxidation of methane and heavy oils, natural gas catalytic decomposition, thermal decomposition of H_2S, thermolysis and electrolysis. However, thermolysis and electrolysis are highly energy intensive [62, 63]. Simultaneous hydrogen production and use is commercially of a great interest due to elimination of storage and transportation steps. Dehydrogenation of hydrocarbons and in-situ hydrogen separation using hydrogen perm-selective membranes is currently state of the art [59, 64, 65].

1.6. Literature Review

Up until now, different researchers have studied both single-step and two-step routes of DME production in heat exchanger reactors. Single-step production of DME inside dehydrogenation of cyclohexane in a heat exchanger reactor was numerically studied by Vakili *et al*.. Enhanced conversion in smaller dimensions of reactor, production of valuable by products *e.g*. hydrogen and benzene and lower temperature of the output streams are advancements of their study. In the next studies, they improved hydrogen and DME production rate by changing flow direction and utilizing a hydrogen perm-selective membrane in an optimized heat exchanger reactor [17, 66, 67]. Simultaneous production of DME, methanol and hydrogen in a thermally double-coupled heat exchange reactor was numerically studied by Farniaei *et al*. and Rahimpour *et al*. They claimed to obtain higher methanol, DME and hydrogen production rates in their new system [59 65]. Farsi *et al*. and

Samimi *et al*. proposed different thermally coupled configurations for methanol dehydration to DME inside various endothermic reactions *e.g*. dehydrogenation of cyclohexane and methyl cyclohexane [68-70]. Goosheneshin *et al*. have made effort to propose a recuperative reactor for simultaneous methanol production and utilization for methyl formate synthesis in a looped heat exchanger reactor. Produced methanol in the exothermic side was suggested to recycle and used for MF production in the endothermic side [71]. In our previous study, we presented a new configuration for production of DME, MF and hydrogen from methanol in thermally coupled membrane reactor. The interesting feature of that configuration was production of various value added products from a single feedstock. We made effort to obtain higher methanol conversion in both sides and hydrogen production in the endothermic side with numerical sensitivity analysis [72].

1.7. Objectives

The present study aims to investigate a thermally coupled reactor equipped with two perm-selective membranes to produce single-step DME, MF, hydrogen and water vapor. In this regard, a heat exchanger reactor with three concentric pipes is proposed. Single-step production of DME from syngas is the exothermic reaction being coupled with methanol dehydrogenation to MF, which is an endothermic reaction. A part of the generated heat in the exothermic side is transferred to the endothermic side through the reactor wall. A membrane with high water perm-selectivity is utilized to separate water in the exothermic side. In addition to this, produced hydrogen in the endothermic side is separated utilizing a hydrogen perm-selective membrane. In-situ reaction and separation can reduce costs of next separation steps and reduce energy consumption. In order to show the performance of system, a mathematical model based on reasonable assumptions is proposed. Genetic Algorithm (GA) method as a powerful optimization technique was applied to obtain optimum values of the operating conditions. Then, a system with higher performance and efficiency is presented.

2. PROCESS DESCRIPTION

2.1. Conventional Single-Step DME Reactor (CSDR)

Hu *et al*. investigated a water-cooled shell and tube fixed bed reactor for single-step production of DME [46-49]. Figure **1** shows a schematic diagram of single-step production of DME. Hybrid catalyst is loaded to the tube side. Boiling water flowing in the shell side works as a coolant. Characteristics of the catalyst and reactor specifications are presented in Table **1**.

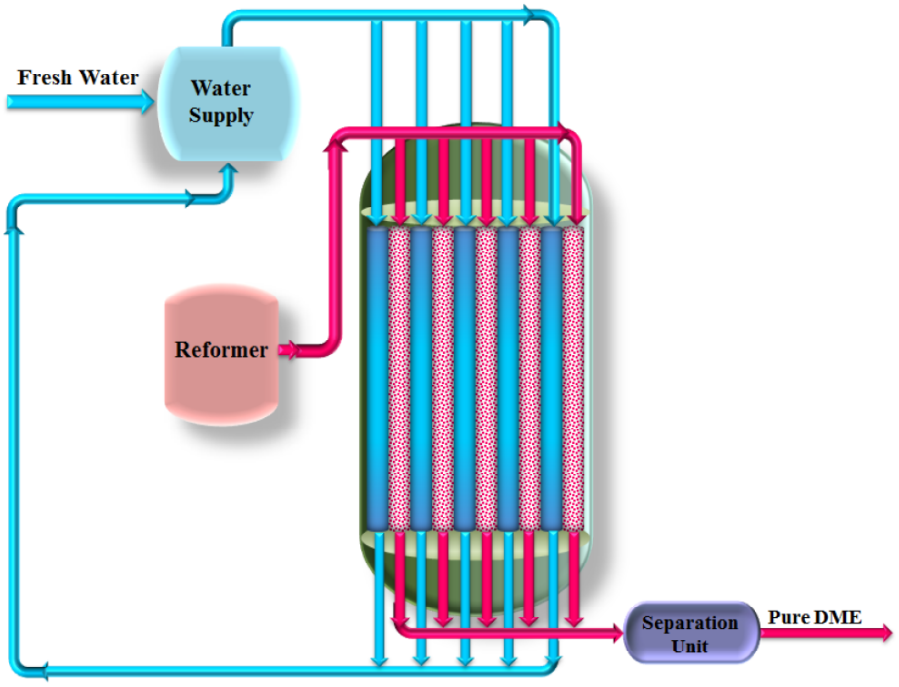

Figure 1: Schematic diagram of single-step production of DME (CSDR).

Table 1: Operating Conditions for the Typical CSDR Process and the Catalyst Characteristics

Parameter	Value	Unit
Feed Composition (Mole Fraction)		
MeOH	0.0030	-
DME	0.0018	-
H_2O	0.0002	-
CO	0.1716	-
CO_2	0.0409	-
H_2	0.4325	-
CH_4	0.0440	-
N_2	0.3160	-
Total molar flow rate of the reactor	0.5542	$mol.s^{-1}$
Inlet temperature	493	K
Inlet pressure	50×10^{5}	Pa
Reactor diameter	38×10^{-3}	m
Reactor length	5.8	m
wall thermal conductivity	48	$J.m^{-1}.K^{-1}.s^{-1}$
Catalyst Particle		
Particle diameter	5×10^{-3}	m
Bed void fraction	0.455	-
Density of catalyst bed	1200	$kg.m^{-3}$

2.2. Thermally Coupled Heat Exchanger Reactor (THR)

Figure **2** shows a conceptual schematic of a two concentric THR configuration with co-current feed flows. Same as CSDR, the tube side is filled with the hybrid catalyst but the shell side is filled with copper-chromite catalyst for methanol dehydrogenation to MF with an endothermic reaction. Thereupon, the endothermic reaction works as a cooling medium. Removing part of the generated heat in DME synthesis side proceeds DME reaction an also drives the MF synthesis reaction. Operating conditions for the endothermic side and associated catalyst characteristics are summarized in Table **2** [72].

2.3. Thermally Coupled Double Membrane Heat Exchanger Reactor (TMHR)

A conceptual schematic of a three concentric TMHR configuration with co-current sweep gases are depicted in Figure **3**. On the outer surface, a Pd/Ag membrane is devised for separation of produced hydrogen in the endothermic side while the inner surface is equipped with a hydroxy sodalite (H-SOD) membrane for separation of produced water in the exothermic side. Water elimination from the exothermic side leads to reaction shifting toward products, more DME production and more heat generation. The results of

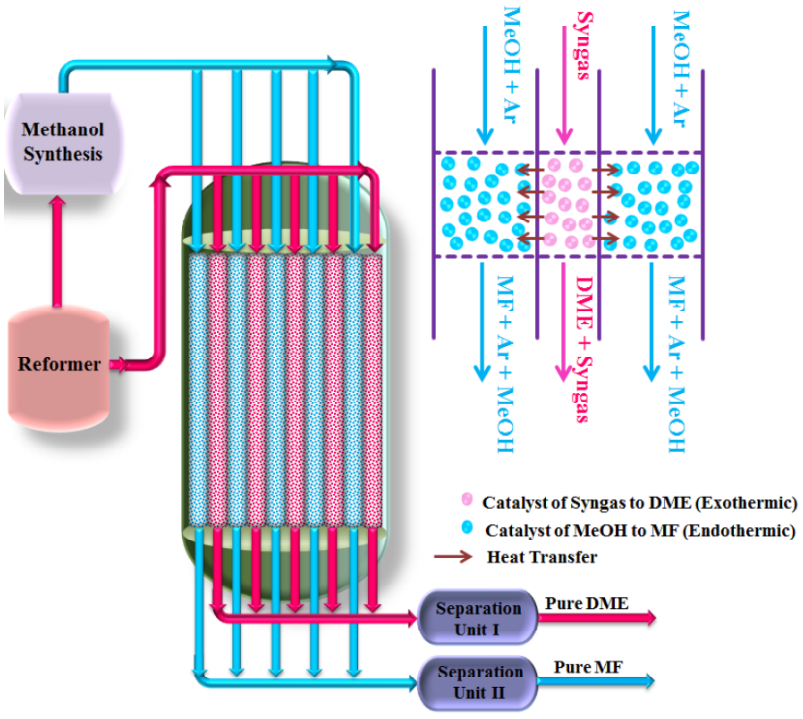

Figure 2: Conceptual schematic of THR configuration with co-current feed flows.

Table 2: Typical Operating Conditions for the Methanol Dehydrogenation in THR

Parameter	Value	Unit
Feed Composition (Mole Fraction)		
MeOH	0.1	-
MF	0	-
H_2	0	-
Ar	0.9	-
Total Molar Flow Rate	0.139	$mol.s^{-1}$
Inlet Temperature	510	K
Inlet Pressure	5×10^{5}	Pa
Catalyst Particle		
Density	4500	$kg.m^{-3}$
Particle Diameter	3.55×10^{-3}	m
Bed Void Fraction	0.39	-
Density of Catalyst Bed	2745	$kg.m^{-3}$

removing hydrogen from the endothermic side are higher methanol conversion, more MF production and higher heat removal from the exothermic side. Dimensions of THR and TMHR are given in Table **3**.

Table 3: Dimensions of THR and OTMHR

Parameter	Value	Unit
THR		
Inner tube (Syngas to DME) diameter	3.8×10^{-2}	m
Shell (MeOH to MF) diameter	8.0×10^{-2}	m
OTMHR		
Inner permeation side diameter	5.0×10^{-2}	m
Inner tube (Syngas to DME) diameter	7.0×10^{-2}	m
Middle tube (MeOH to MF) diameter	10.5×10^{-2}	m
Outer permeation side diameter	15.0×10^{-2}	m
Length of the reactor	5.8	m

3. REACTION SCHEMES AND KINETICS

3.1. Syngas to DME

Followings are independent reactions occurring on the hybrid catalyst for single-step DME production from syngas [46-49]:

$$CO + 2H_2 \rightleftarrows CH_3OH \qquad \Delta H_{298} = -90.55\ \frac{kJ}{mol} \qquad (1)$$

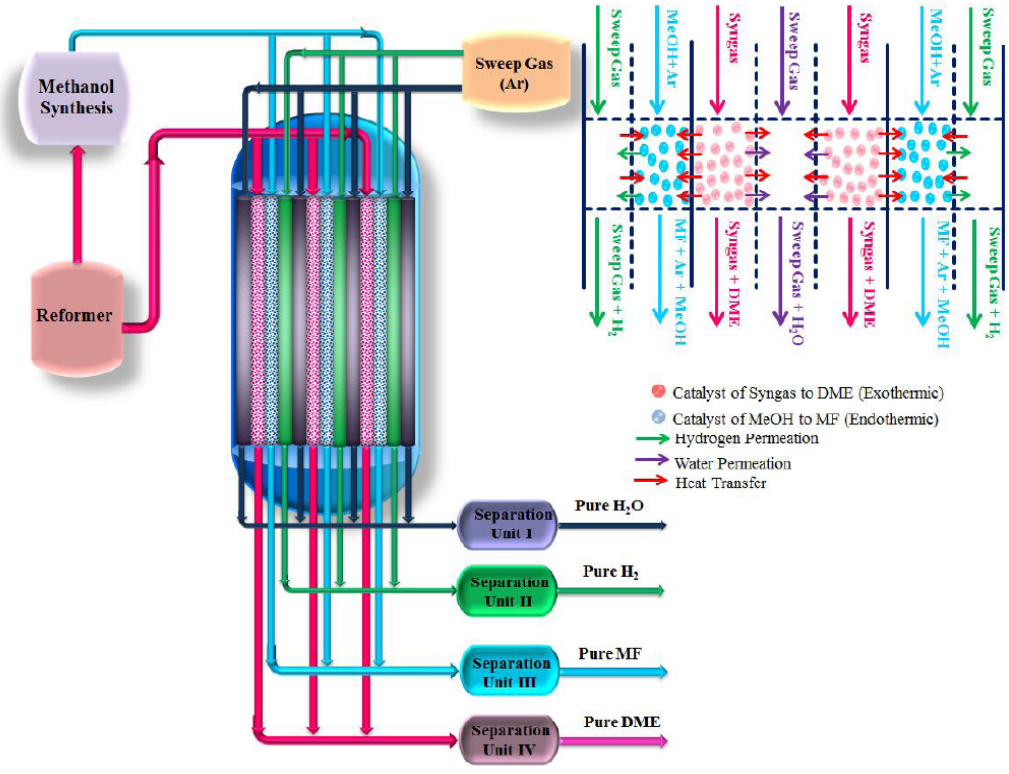

Figure 3: Conceptual schematic of TMHR configuration with co-current sweep gases.

$$CO_2 + 3H_2 \rightleftarrows CH_3OH + H_2O \qquad \Delta H_{298} = -49.43 \frac{kJ}{mol} \tag{2}$$

$$2CH_3OH \rightleftarrows CH_3OCH_3 + H_2O \qquad \Delta H_{298} = -21 \frac{kJ}{mol} \tag{3}$$

Obviously, water is a side product of these reactions. Reactions 1-3 are all exothermic and equilibrium. Following expressions were proposed for reaction kinetics [46-49]:

$$r_{CO} = \frac{k_1 f_{CO} f_{H_2}^2 (1-\beta_1)}{\left(1 + K_{CO} f_{CO} + K_{CO_2} f_{CO_2} + K_{H_2} f_{H_2}\right)^3} \tag{4}$$

$$r_{CO_2} = \frac{k_2 f_{CO_2} f_{H_2}^3 (1-\beta_2)}{\left(1 + K_{CO} f_{CO} + K_{CO_2} f_{CO_2} + K_{H_2} f_{H_2}\right)^4} \tag{5}$$

$$r_{DME} = \frac{k_3 f_{CH_3OH} (1-\beta_3)}{\left(1 + \sqrt{K_{CH_3OH} f_{CH_3OH}}\right)^2} \tag{6}$$

$$\beta_1 = \frac{f_{CH_3OH}}{K_{eq,1} f_{CO} f_{H_2}^2} \tag{7}$$

$$\beta_2 = \frac{f_{CH_3OH} f_{H_2O}}{K_{eq,2} f_{CO_2} f_{H_2}^3} \tag{8}$$

$$\beta_3 = \frac{f_{DME} f_{H_2O}}{K_{eq,3} f_{CH_3OH}^2} \tag{9}$$

Reaction rate constants (k_i), adsorption constants (K_i) and equilibrium constants ($K_{eq,i}$) are summarized in Table **4** [46-49].Peng-Robinson equation of state (PR EOS) is used to calculate the fugacities of components. PR EOS, corresponding correlations, fugacity equations and critical properties of the components are presented in **Appendix A**.

3.2. Methanol Dehydrogenation to MF

Methanol is dehydrogenated to MF with an endothermic equilibrium reaction:

$$2CH_3OH \rightleftarrows CH_3OCHO + 2H_2 \qquad \Delta H_{298} = 98.9 \frac{kJ}{mol} \tag{10}$$

Following rate expression was proposed by Huang *et al*. for methanol dehydrogenation to MF on a commercial copper-chromite catalyst [71-73]:

$$r_{MeOH} = \frac{-k_2 K_{21}^{0.5} f_{CH_3OH} f_{H_2}^{-0.5}}{\left(1 + K_{21} K_{24}^{0.5} f_{CH_3OH} f_{H_2}^{-0.5} + K_{23}^{-1} f_{CH_3OCHO} + K_{22}^{-0.5} K_{23}^{-0.5} f_{CH_3OCHO}^{0.5} + K_{24}^{-0.5} f_{H_2}^{-0.5}\right)^2} \tag{11}$$

Table 4: Rate Constants, Adsorption Constants and Equilibrium Constants of Syngas to DME Reaction Rates

$k_i = k_{0,i} exp\left(-\frac{A}{RT}\right)$		
Rate Constant	**$k_{0,i}$**	**A**
k_1	1.8280×10^3 (mol.kg^{-1}.s^{-1}.bar^{-3})	43723 (J.mol^{-1}.K^{-1})
k_2	0.4195×10^2 (mol.kg^{-1}.s^{-1}.bar^{-4})	30253 (J.mol^{-1}.K^{-1})
k_3	1.9390×10^2 (mol.kg^{-1}.s^{-1}.bar^{-1})	24984 (J.mol^{-1}.K^{-1})
$K_i = K_{0,1} exp\left(\frac{E_a}{RT}\right)$		
Adsorption Constant	**$K_{0,i}$**	**E_a**
K_{CO}	8.252×10^{-4} (bar^{-1})	30275 (J.mol^{-1}.K^{-1})
K_{CH3OH}	1.726×10^{-4} (bar^{-1})	60126 (J.mol^{-1}.K^{-1})
K_{CO2}	2.100×10^{-3} (bar^{-1})	31846 (J.mol^{-1}.K^{-1})
K_{H2}	0.1035 (bar^{-1})	-11139 (J.mol^{-1}.K^{-1})

$\ln K_{eq,i} = A + \frac{B}{T} + C \ln T + DT + ET^2 + FT^3 + GT^4$							
Eq. Constant	A	B	C	D×10^2	E×10^4	F×10^8	G×10^{11}
$K_{eq,1}$(atm^{-2})	13.1652	9203.26	-5.92839	-0.352404	0.102264	-0.769446	0.238583
$K_{eq,2}$(atm^{-2})	1.6654	4553.34	-2.72613	-1.106294	0.172060	-1.106294	0.319698
$K_{eq,3}$(-)	-9.3932	3204.71	0.83593	0.235267	-0.018736	0.051606	0

Where, k_2=0.43 mol.gr^{-1}.hr^{-1}, K_{21}=0.48×10^{-5} Pa^{-1}, K_{22}=3.66×10^3 Pa, K_{23}=0.6×10^3 Pa and K_{24}=30×10^3 Pa. It should be mentioned that they proposed the rate equation in terms of partial pressures. In order to account the non-ideality of the gaseous mixture, we applied the rate equation in terms of fugacities.

4. MATHEMATICAL MODELING

4.1. Governing Equations

Following assumptions are applied to develop a proper mathematical model to evaluate performance of the proposed heat exchanger reactors:

- Homogeneous reactions in both exothermic and endothermic sides
- Neglecting radial gradient in reaction and membrane sides and plug flow pattern (one-dimensional initial value model)
- Steady state condition in reaction and membrane sides
- Bed symmetry in both sides due to constant porosity
- Adiabatic operation (no heat loss from inside and outside of the reactor)
- Non-ideal gaseous mixtures
- Ergun equation for pressure drop in the reaction side
- No pressure drop in the permeation sides

Table 5: Governing Equations and Boundary Conditions

Definition	Equation	
Mass Balance		
Exothermic side	$\frac{-1}{A_{c,1}}\frac{dF_{i,1}}{dz}+\eta\rho_{B,1}r_{i,1}-\beta_1\frac{\pi D_1}{A_{c,1}}J_{H_2O}=0\ ;\ \beta_1=1\ for\ H_2O\ else\ \beta_1=0$	(12)
Endothermic Side	$\frac{-1}{A_{c,2}}\frac{dF_{i,2}}{dz}+\eta\rho_{B,2}r_{i,2}-\beta_2\frac{\pi D_2}{A_{c,2}}J_{H_2}=0\ ;\ \beta_2=1\ for\ H_2\ else\ \beta_2=0$	(13)
Inner Permeation Sides	$-\frac{dF_{i,j}}{dz}+\varphi_1\pi D_j J_{H_2O}=0\ ;\ \varphi_1=1\ for\ H_2O\ else\ \varphi_1=0$	(14)
Outer Permeation Sides	$-\frac{dF_{i,j}}{dz}+\varphi_2\pi D_j J_{H_2}=0\ ;\ \varphi_2=1\ for\ H_2\ else\ \varphi_2=0$	
Energy Balance		
Exothermic side	$\frac{-C^g_{p,1}}{A_{c,1}}\frac{d\left(F_{t,1}T_1\right)}{dz}+\rho_{B_1}\sum_{i=1}^{NC}\eta r_{i,1}\left(-\Delta H_{f,i}\right)-\frac{\pi D_1}{A_{c,1}}U(T_1-T_2)-J_{H_2O}\left(T_1-T_{p,in}\right)=0$	(15)
Endothermic Side	$\frac{-C^g_{p,2}}{A_{c,2}}\frac{d\left(F_{t,2}T_2\right)}{dz}+\rho_{B_2}\sum_{i=1}^{NC}\eta r_{i,2}\left(-\Delta H_{f,i}\right)-\frac{\pi D_2}{A_{c,2}}U(T_2-T_1)-J_{H_2}\left(T_2-T_{p,out}\right)=0$	(16)
Inner Permeation Sides	$-C^g_{p,l}\frac{d\left(F_{t,p,l}T_{p,l}\right)}{dz}+\pi D_l J_{H_2O}\int_{T_{p,l}}^{T_j}C^g_{p,H_2O}dT+\pi D_j U_j\left(T_j-T_{p,l}\right)=0$	(17)
Outer Permeation Side	$-C^g_{p,l}\frac{d\left(F_{t,p,l}T_{p,l}\right)}{dz}+\pi D_l J_{H_2}\int_{T_{p,l}}^{T_j}C^g_{p,H_2}dT+\pi D_j U_j\left(T_j-T_{p,l}\right)=0$	(18)
Pressure drop		
Pressure drop	$\frac{dp}{dz}=\frac{150\mu}{\phi_s^2 d_p^2}\frac{(1-\varepsilon)^2}{\varepsilon^3}\frac{Q}{A_c}+\frac{1.75\rho}{\phi_s d_p}\frac{(1-\varepsilon)}{\varepsilon^3}\frac{Q^2}{A_c^2}$	(19)
Boundary conditions		
Reaction Sides Permeation Sides	$z=0\implies F_{i,j}=F_{i,j,0}\ ;\ T_j=T_{j,0}\ ;\ P_j=P_{j,0}\ ;j=1,2$ $z=0\implies F_{i,l}=F_{i,l,0}\ ;\ T_{p,l}=T_{p,l,0}\ ;l=3,4$	(20)

As a result, a set of ordinary differential equations (ODEs) is obtained considering an axial differential element. The governing equations with associated boundary conditions are tabulated in Table **5**. Auxiliary correlations to determine thermophysical properties and heat transfer coefficients are presented in **Appendix B**.

4.1. Water Separation Via Hydroxy Sodalite (H-SOD) Membrane

H-SOD is a zeolite like material with high water perm-selectivity and thermal/mechanical stability at high temperatures and pressures. H-SOD membranes have found applications in separation of compounds with small size *e.g*. water (kinetic diameter of water molecule is 2.68 A˚). Rohde *et al*. reported that H-SOD membranes are almost 100 % selective to water in the mixtures containing hydrogen and carbon monoxide. Hence, in-situ water removal from DME production side by using an H-SOD membrane layer is state of art. Following equation is considered to account water permeation rate [31-34]:

$$J_{H_2O} = \frac{Q_{H_2O} A_s}{V_r} \left(P_{H_2O,1} - P_{H_2O,4}\right) \quad (21)$$

Where, A_s is the surface area Q_{H_2O} is permeance of water (1-10×10^{-7} mol.s^{-1}.m^{-2}.Pa^{-1}) and V_r is reactor volume. , $P_{H_2O,j}$ and $P_{H_2O,m}$ are water partial pressures in the reaction and permeation sides, respectively.

4.3. Hydrogen Permeation Via Palladium/Silver Membrane

Membranes composited of palladium are widely used for purification of hydrogen in the hydrogen containing mixtures. Promoters such as silver are added to the palladium alloys to enhance hydrogen perm-selectivity [74-76]. Regarding perm-selectivity of this composite, a continuous thin layer (6 μm) of Pd/Ag alloy is equipped on the surface of a thermo-stable support and subjected to the hydrogen rich stream. The hydrogen permeation rate is assumed to follow the Sieverts' law in which Q_0 =1.65×10^{-5} mol.m^{-1}.s^{-1}.kPa$^{-0.5}$ and ,E-,H-2..=15.7 kJ., mol-−1.[77, 78]:

$$J_{H_2} = \frac{Q_0}{\delta_{H_2}} exp\left(-\frac{E_{H_2}}{RT}\right)\left(\sqrt{P_{H_2,2}} - \sqrt{P_{H_2,3}}\right) \quad (22)$$

$P_{H_2,j}$ and $P_{H_2,m}$ are partial pressures of hydrogen in the reaction and permeation sides, respectively and δ_{H_2} is the membrane thickness.

5. NUMERICAL SOLUTION AND OPTIMIZATION

5.1 Numerical Solution

The obtained mathematical model is a set of equations consisted of ODEs, associating boundary conditions, auxiliary correlations for thermophysical properties and fugacity equations. Backward scheme of finite difference method was used to convert the set of ODEs to a set of nonlinear algebraic equations coupled with other equations. Length of the reactor was divided to 100 grids to obtain a low numerical error and stable solution. The obtained set of nonlinear algebraic equations in each section was solved in MATLAB media. The output of each grid was considered as an initial guess to solve the equations in the next grid. Simulation results obtained in the present study are compared with those of Hu *et al*. [46] in Table **6**. Based on the obtained errors, the proposed model is acceptable.

Table 6: Comparison between Simulation Results and Results of Hu *et al*.

Conventional Single-Step DME Reactor			
Output	**Simulation**	**Hu *et al.* [46]**	**Relative Error %**
Output CO mole fraction	0.0850	0.0877	-3.1
Output CO_2 mole fraction	0.0642	0.0671	-4.32
Output DME mole fraction	0.0451	0.0491	-8.14
Output temperature (K)	513.88	516.75	-0.55

5.2 Optimization

An optimization procedure is applied to find the optimum values of certain decision variables leading to maxima or minima in the appropriate objective functions. On the other side, higher productivity and efficiency is managed by determining optimum operating conditions [79]. In this research, we aim to maximize carbon monoxide, carbon dioxide and hydrogen conversion to DME in the exothermic side, methanol conversion to MF in the endothermic side, hydrogen recovery yield and DME molar fraction in the product of the exothermic side, simultaneously. The aforementioned parameters are defined as following:

Carbon monoxide conversion: $X_{CO} = \frac{F_{CO,in} - F_{CO,out}}{F_{CO,in}}$ (23)

Carbon dioxide conversion: $X_{CO_2} = \frac{F_{CO_2,in} - F_{CO_2,out}}{F_{CO_2,in}}$ (24)

Hydrogen conversion: $X_{H_2} = \frac{F_{H_2,in,1} - F_{H_2,out,1}}{F_{H_2,in,1}}$ (25)

Methanol conversion: $X_{MeOH,2} = \frac{F_{MeOH,in,2} - F_{MeOH,out,2}}{F_{MeOH,in,2}}$ (26)

Hydrogen recovery yield: $Y_{H_2} = \frac{F_{H_2,m}}{F_{MeOH,in,2}}$ (27)

DME molar fraction: $y_{DME} = \frac{F_{DME,out,3}}{F_{tot,out,3}}$ (28)

In this regard, sum of $X_{CO}, X_{CO_2}, X_{H_2}, X_{MeOH,2}, Y_{H_2}$ and y_{DME} is considered as the objective function:

$$OF = X_{CO} + X_{CO_2} + X_{H_2} + X_{MeOH,2} + Y_{H_2} + y_{DME} \quad (29)$$

Sixteen decision variables are manipulated during optimization procedure. Selected decision variables and their feasible bounds are summarized in Table **7**. A Genetic Algorithmis applied for maximization of the objective function. GA that is simulated form of natural evolution is known as a powerful technique between stochastic methods. Population of possible solutions for the problem is maintained and evolved by exerting stochastic operators in an iterative manner. More details on basic components of GA such as gene, chromosome, population, selection and crossover could be found elsewhere [80, 81]. Obtained optimum values of the decision variables are tabulated in Table **8**.

6. RESULTS AND DISCUSSION

Performance of the optimized thermally coupled double membrane reactor (OTMHR) and THR is discussed in this section. A THR with the characteristics given in Tables **1-3** is considered as a "reference case". Hence, molar and thermal behavior of OTMHR is compared with the reference case.

6.1. OTMHR

In this section, numerical results obtained for OTMHR is discussed. Figure **4** and **5** shows flow rates of components in both reaction sides. As shown in Figure **4**, flow rates of hydrogen and carbon monoxide in the upper section of exothermic side have sharp decrease due to consumption according to reactions 1

Table 7: Decision Variables and Feasible Bounds

Parameter	Feasible Bounds	Unit
Inlet Flow Rate of Exothermic Side	$0.1 \leq F_{t0,1} \leq 0.5$	$mol.s^{-1}$
Inlet Temperature of Exothermic Side	$495 \leq T_{0,1} \leq 523$	K
Inlet Pressure of Exothermic Side	$50 \times 10^5 \leq P_{t0,1} \leq 75 \times 10^5$	Pa
Inlet CO Mole Fraction of Exothermic Side	$0.1 \leq y_{CO,0} \leq 0.3$	-
Inlet CO_2 Mole Fraction of Exothermic Side	$0.01 \leq y_{CO_2,0} \leq 0.1$	-
Inlet H_2 Mole Fraction of Exothermic Side	$0.3 \leq y_{H_2,0} \leq 0.6$	-
Inlet Flow Rate of Endothermic Side	$0.1 \leq F_{t0,2} \leq 0.3$	$mol.s^{-1}$
Inlet MeOH Mole Fraction of Endothermic Side	$0.1 \leq y_{MeOH\ 0,2} \leq 0.3$	-
Inlet Temperature of Endothermic Side	$453 \leq T_{0,2} \leq 523$	K
Inlet Pressure of Endothermic Side	$4 \times 10^5 \leq P_{t0,2} \leq 7 \times 10^5$	Pa
Inlet Flow Rate of Outer Permeation Side	$0.5 \leq F_{m0,outer} \leq 2$	$mol.s^{-1}$
Inlet Temperature of Outer Permeation Side	$500 \leq T_{m0,outer} \leq 543$	K
Inlet Pressure of Outer Permeation Side	$0.05 \times 10^5 \leq P_{t0,outer} \leq 0.1 \times 10^5$	Pa
Inlet Flow Rate of Inner Permeation Side	$0.5 \leq F_{m0,inner} \leq 2$	$mol.s^{-1}$
Inlet Temperature of Inner Permeation Side	$453 \leq T_{m0,inner} \leq 500$	K
Inlet Pressure of Inner Permeation Side	$0.05 \times 10^5 \leq P_{t0,inner} \leq 0.1 \times 10^5$	Pa

Table 8: Optimum Values of the Decision Variables

Parameter	Value	Unit
$F_{t0,1}$	0.1019	mol.s^{-1}
$T_{0,1}$	503.1	K
$P_{0,1}$	74.706×10^5	Pa
$y_{CO,0}$	0.1076	-
$y_{CO_2,0}$	0.0388	-
$y_{H_2,0}$	0.4981	-
$F_{t0,2}$	0.1181	mol.s^{-1}
$y_{MeOH\ 0,2}$	0.1048	-
$T_{0,2}$	453.3	K
$P_{0,2}$	5.166×10^5	Pa
$F_{m0,outer}$.	1.4774	mol.s^{-1}
$T_{0,outer}$	503.1	K
$P_{0,outer}$	0.059×10^5	Pa
$F_{m0,inner}$.	1.4817	mol.s^{-1}
$T_{0,inner}$.	503.2	K
$P_{0,inner}$.	0.071×10^5	Pa

and 2. Then, they reach to a constant value in the lower section of the reactor. DME shows an ascending trend in the upper section followed by a constant value in the lower section of the reactor. Such trends are due to the reached chemical equilibrium in the lower section. Carbon monoxide, carbon dioxide, methanol and water show different behaviors. Both methanol and water have a maximum point in the reactor entrance. However, location of maximum point in water profile does not coincide with that of methanol. This is due to different basis beyond these phenomena. Simultaneous methanol consumption and water production according to reaction 3 is also effective in such an observation. In addition to this, methanol is produced according reactions 1 and 2. Hence, its profile shows an ascending trend in the beginning. DME production according to reaction 3, leads to immediate consumption of methanol. Hence, methanol flow rate starts to fall after a maximum point. Water is produced according equations 2 and 3 in the reactor entrance. As soon as water accumulates, it is separated by the inner membrane. In fact, rate of water permeation overcomes rate of water production in this point. Hence, presence of maximum point in the water profile is justifiable. Carbon dioxide is converted to methanol and water according reaction 2. Methanol converting to DME and water separation lead to higher carbon dioxide consumption. Due to equilibrium nature of the reactions, water separation from reaction medium leads to more DME production.

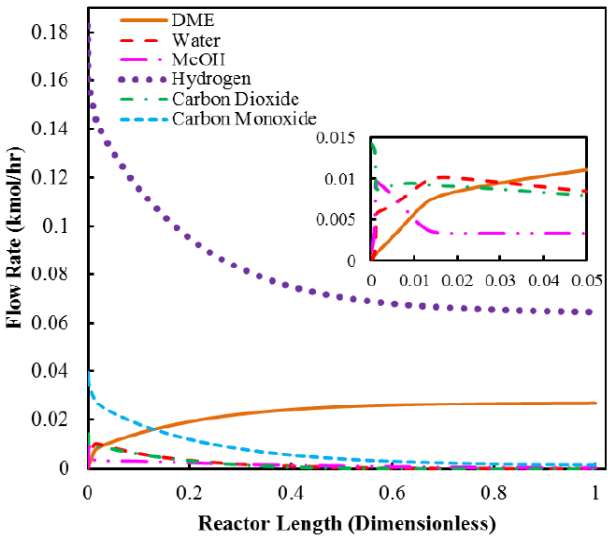

Figure 4: Flow rates of components in the exothermic side of OTMHR.

Figure **5** shows flow rates of methanol, MF and hydrogen in the endothermic side of OTMHR.A gradual decrease in methanol flow rate and a gradual increase in MF flow rate are observed while trend of hydrogen flow rate is different. As shown, hydrogen flow rate shows an immediate increase in the upper section due to production according reaction 10. Hydrogen permeation through the outer membrane leads to

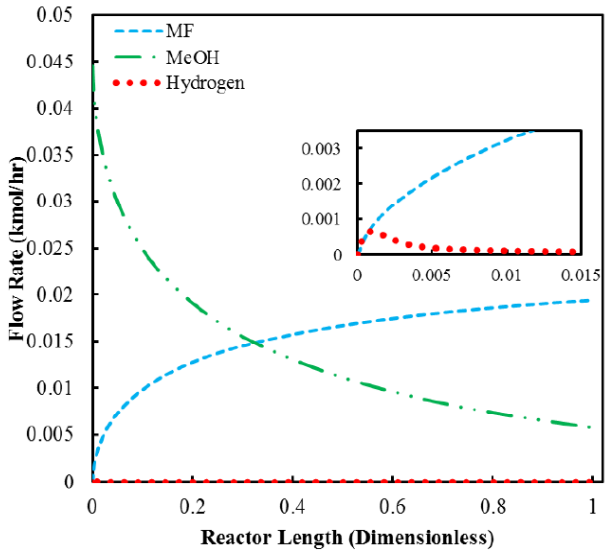

Figure 5: Flow rates of components in the endothermic side of OTMHR.

hydrogen decrease. In this point of reactor, rate of hydrogen permeation overcomes rate of hydrogen production. Hence, produced hydrogen is totally separated in the whole length of reactor. Separation of hydrogen makes the reaction shift toward more methanol consumption, more MF production and then higher purity of output stream.

Methanol conversion to MF in the endothermic side as well as hydrogen, carbon monoxide and carbon dioxide conversions in the exothermic side are compared in Figure **6**. Methanol conversion to MF in the endothermic side has an ascending trend. While hydrogen, carbon monoxide and carbon dioxide conversion profiles are a bit different in the reactor entrance. Clearly, carbon dioxide and carbon monoxide are almost entirely converted.

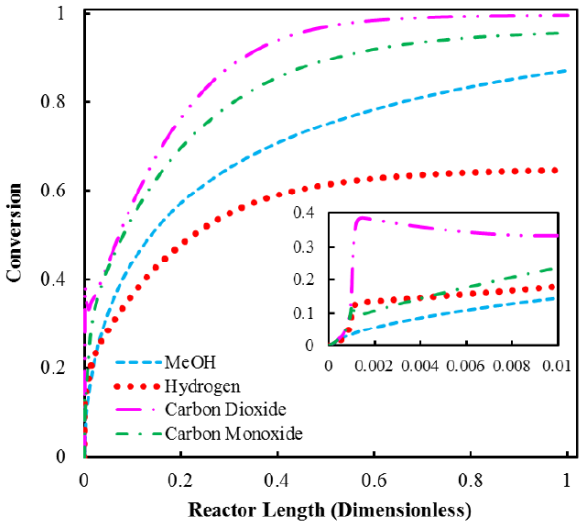

Figure 6: Methanol conversion to MF in the endothermic side and hydrogen, carbon monoxide and carbon dioxide conversions in the exothermic side, OTMHR.

Axial temperature profiles of reaction sides and permeation sides are presented in Figure **7**. A hot point in the upper section of both reaction sides is observed. However, the exothermic side reaches higher temperature. In this point, rate of heat transfer from the exothermic side to the endothermic side and inner membrane side overcomes rate of heat generation by the exothermic reactions. The hot point in the endothermic side is a result of contest between rate of heat transfer from the exothermic and outer membrane sides and rate of heat consumption by the endothermic reaction. Consequently, at this point, rate of heat consumption overcomes rate of heat transfer. Temperature profile of the inner permeation side (which is inside the exothermic side) is similar to the exothermic side while temperature profile of outer permeation side (which is inside the endothermic side) is different with that of endothermic side. All the streams tend to become isothermal in the output of the reactor. Such an observation may be due to probable established chemical equilibrium in the reaction sides. On the other hand, at the equilibrium, reactions are terminated and heat generation and consumption processes are inevitably stopped.

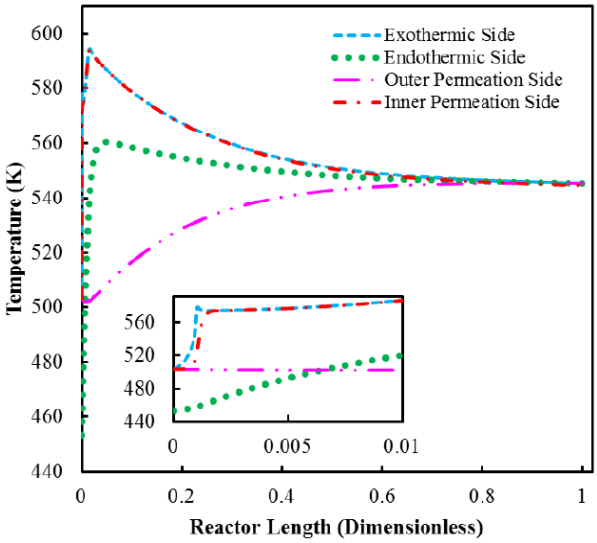

Figure 7: Axial temperature profiles of reaction sides and permeation sides, OTMHR.

Axial pressure profiles of the reaction sides are compared in Figure **8**. Both sides show a nearly linear pattern for pressure variations. The exothermic side shows 0.02 bar (% 0.03) pressure drop while the pressure drop in endothermic side is 0.63 bar (% 12.24). Different dimensions, different physical properties of reacting mixtures such as viscosity and

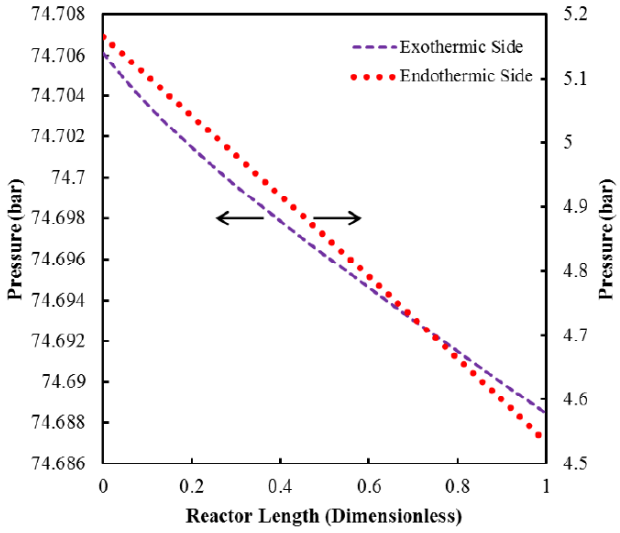

Figure 8: Axial pressure profiles of the reaction sides, OTMHR.

density and different permeation rates from the reaction sides are main reasons for different pressure drops in two sides.

Molar behaviors and recoveries of inner and outer permeation sides are shown in Figure **9** and **10**. As per Figure **9**, hydrogen mole fraction in the outer permeation side and water mole fraction in the inner permeation side have both ascending trends. However, their behaviors in the beginning of the reactor are different. Hydrogen permeation begins right from the reactor inlet while water permeation begins after a short distance from the reactor inlet. In fact, contest of permeation rates and component production by the reactions have strong influences on profiles of hydrogen and water in the membrane sides as well as reaction sides.

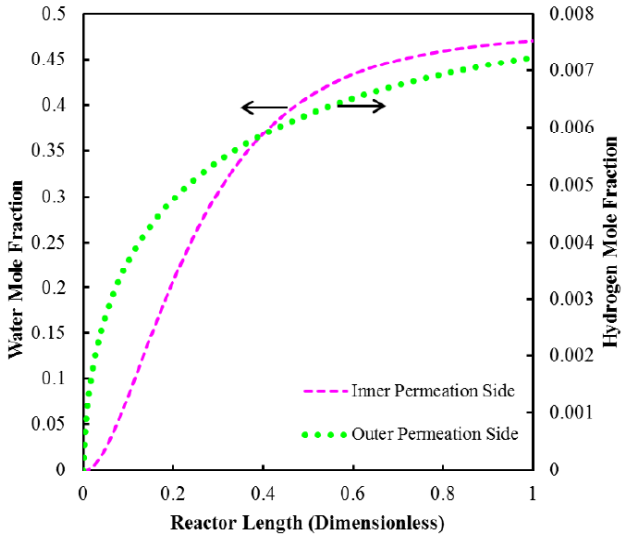

Figure 9: Water and hydrogen mole fractions in the inner and outer permeation sides, OTMHR.

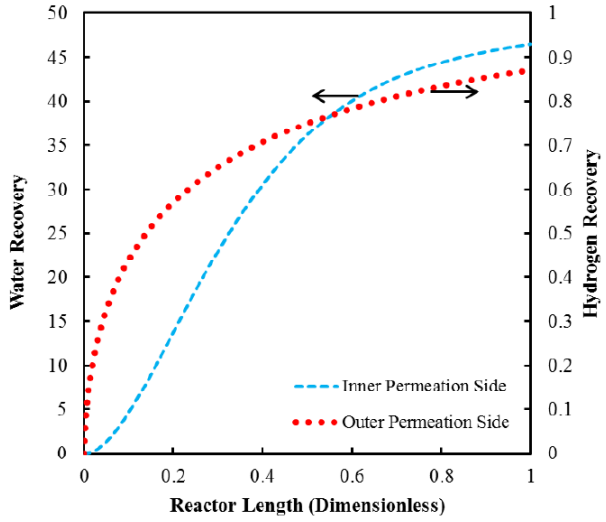

Figure 10: Water and hydrogen recoveries in the inner and outer permeation sides, OTMHR.

6.2. OTMHR Vs. THR

In order to have a better understanding of facilities provided by the proposed configuration, a comparison between OTMHR and THR is presented in this section.

Thermal behavior of OTMHR and THR are compared in Figure **11**. Isothermal output streams in both THR and OTMHR configurations are obtained. However, product streams of THR have higher temperature in both reaction sides. Lower output temperatures of OTMHR may be due to presence of permeation sides. On the one hand, a part of generated heat by the exothermic reactions is transferred to the permeation sides and is spent to warm up the permeation side streams. This leads to output streams with lower temperature. Reacting mixtures with lower temperature reduces the probability of catalyst sintering or destruction. As can be seen in Figure **11**, hot point in the exothermic side of OTMHR has higher temperature, while hot point in the endothermic side of THR shows higher temperature. Presence of permeation sides and different operating conditions in the feed of reactors strongly affect the thermal behavior and temperature pattern of the reactors.

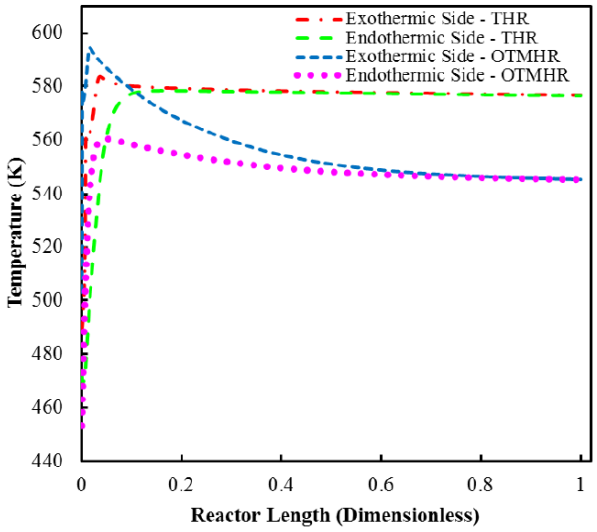

Figure 11: Comparing axial temperature profiles of both exothermic and endothermic sides in THR and OTMHR.

Figures **12-15** give an overview of molar behavior of THR and OTMHR. Hydrogen flow rates and conversions in THR and OTMHR are compared in Figure **12**. Clearly, higher hydrogen conversion in OTMHR is obtained. Higher heat transfer rate from the exothermic side as well as water elimination from

reaction medium is the reason of such an improvement. Figure **13** is to compare carbon monoxide flow rates and conversions in THR and OTMHR. An evident improvement in conversion of carbon monoxide due to higher heat transfer and water separation is obtained. A comparison between methanol conversions and flow rates in the endothermic side of THR and OTMHR is presented in Figure **14**. As per figure, elimination of hydrogen from this side by using a membrane leads to higher methanol conversion. Production rates of DME and MF as the main products of the proposed configuration in THR and OTMHR are compared in Figure **15**. Equipping membranes inside both reaction sides makes enhancement in production rates.

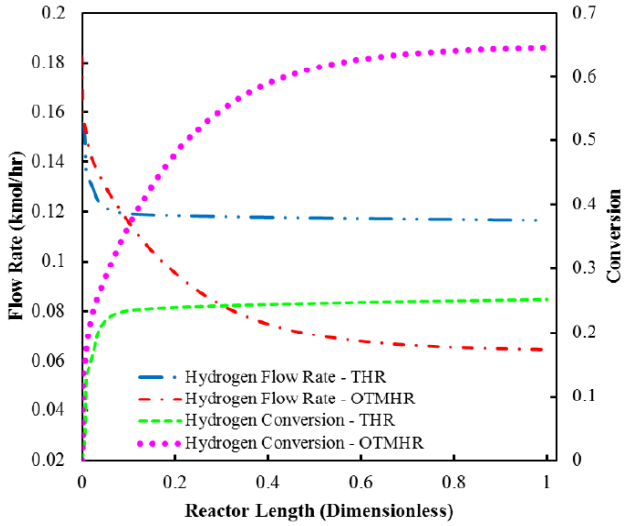

Figure 12: Comparing hydrogen flow rates and conversions in the exothermic sides of THR and OTMHR.

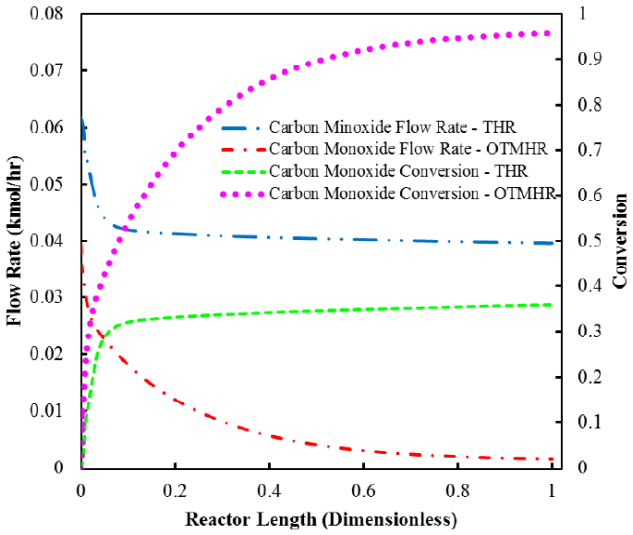

Figure 13: Comparing carbon monoxide flow rates and conversions in the exothermic sides of THR and OTMHR.

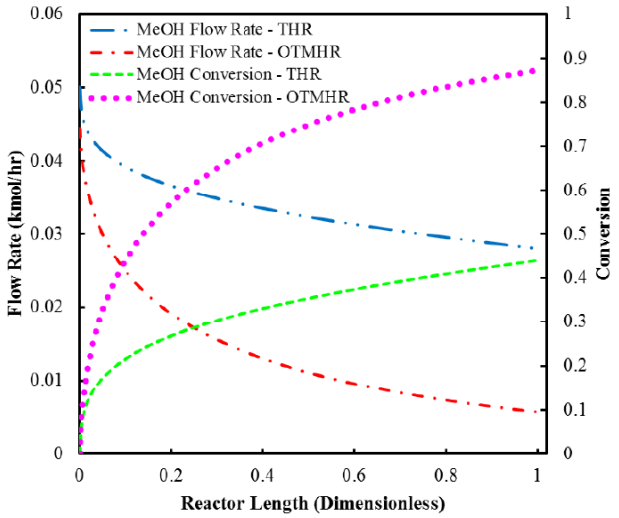

Figure 14: Comparing MeOH flow rates and conversions in the endothermic sides of THR and OTMHR.

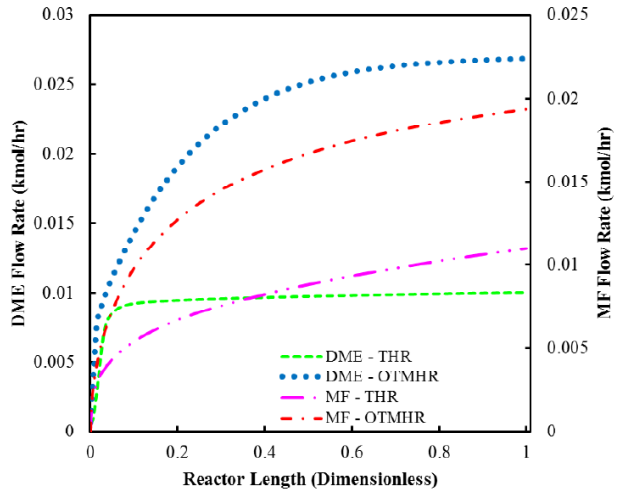

Figure 15: Comparing MF and DME production rates of THR and OTMHR.

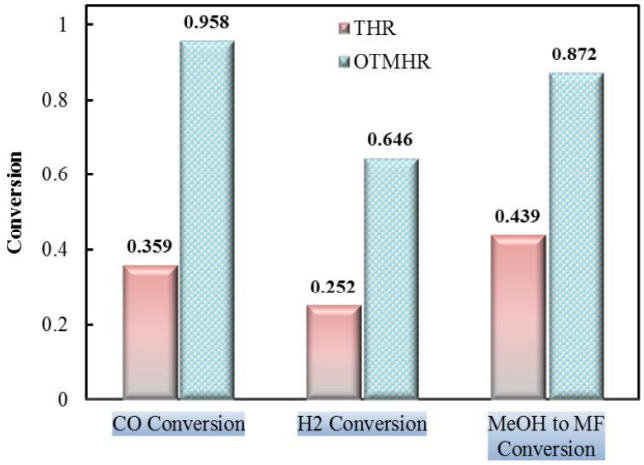

Figure 16: Comparing output conversions of exothermic and endothermic sides in THR and OTMHR.

Output conversions of exothermic and endothermic sides in THR and OTMHR are presented in Figure **16**. Carbon monoxide and hydrogen conversions show %60 and % 39 improvement, respectively, while methanol to MF conversion shows % 44improvement. As a whole, higher production rate of desired products and lower output temperature are obtained by using the double assisted membrane reactor.

7. CONCLUSION

DME production from syngas and MF/hydrogen production from methanol in a catalytic heat-exchanger reactor equipped with two membranes was studied numerically.DME synthesis from syngas plays the role of heat source for driving the endothermic reaction *i.e*. methanol dehydrogenation. Followings are achieved with using the proposed configuration:

- Reducing energy consumption by direct achieving autothermality in the reactor
- Efficient energy separations with the membranes
- Producing various products in a single system
- Achieving higher DME and MF production rates
- Recovery of pure hydrogen and water vapor
- Output streams with lower temperature leading to reducing risk of catalyst destruction

Utilizing OTMHR configuration promotes CO conversion to % 95.8, H_2 conversion to % 64.6 and methanol conversion to MF to % 87.2. Besides, comparing with THR, % 60 increase in CO conversion, % 39 increase in H_2 conversion and % 43 increase in methanol conversion to MF was achieved using the optimized thermally coupled double membrane heat exchanger reactor.

ACKNOWLEDGEMENTS

The authors are grateful to the Shiraz University for supporting this research.

NOMENCLATURE

A_c	cross-section area, m^2
A_i	inside area of inner tube, m^2
A_o	outside area of inner tube, m^2
c_1, c_2, c_3, c_4, c_5	constants of the specific heat correlation
Cp	specific heat of the gas at constant pressure, $J.mol^{-1}.K$
d_p	particle diameter, m
D_i	tube inside diameter, m
D_o	tube outside diameter, m
D_j	diameter of each side, m
E_{H2}	activation energy in hydrogen permeation rate model, $kJ.mol^{-1}$
f_i	fugacity of component i, Pa
F_i	molar flow rate of the components, $mol.s^{-1}$
F_t	total molar flow rate, $mol.s^{-1}$
h_i	heat transfer coefficient between fluid phase and reactor wall in the exothermic side, $W.m^{-2}.K^{-1}$
h_o	heat transfer coefficient between fluid phase and reactor wall in the endothermic side, $W.m^{-2}.K^{-1}$
$\Delta H_{f,i}$	enthalpy of formation of component i, $J.mol^{-1}$
J_{H2}	hydrogen permeation flux, $mol.m^{-2}.s^{-1}$
J_{H2O}	water permeation flux, $mol.m^{-3}.s^{-1}$
k_1	rate constant of DME synthesis reaction, $mol.kg^{-1}.s^{-1}.bar^{-3}$
k_2	rate constant of DME synthesis reaction,$mol.kg^{-1}.s^{-1}.bar^{-4}$
k_3	rate constant of DME synthesis reaction,$mol.kg^{-1}.s^{-1}.bar^{-1}$
K_{CO}, K_{CO2}, K_{H2}, K_{CH3OH}	adsorption constants of DME synthesis reaction, atm^{-1}
$K_{eq,1}$	equilibrium constant of DME synthesis reaction, atm^{-2}
$K_{eq,2}$	equilibrium constant of DME synthesis reaction, atm^{-2}
$K_{eq,3}$	equilibrium constant of DME synthesis reaction, dimensionless
k_2	rate constant of methanol dehydrogenation reaction, $mol.gr^{-1}.hr^{-1}$
k_{th}	thermal conductivity of the components, $W.m^{-1}.K^{-1}$
K_{21}	rate constant of methanol dehydrogenation reaction, Pa^{-1}
K_{22}	rate constant of methanol dehydrogenation reaction, Pa
K_{23}	rate constant of methanol dehydrogenation reaction, Pa
K_{24}	rate constant of methanol dehydrogenation reaction, Pa
K_{eq}	equilibrium constant for the methanol dehydration reaction, dimensionless
K_w	thermal conductivity of the reactor wall, $W.m^{-1}.K^{-1}$

L	reactor length, m
MW	molecular weight of component i, $g.mol^{-1}$
NC	number of components (NC=8 for the exothermic side and NC=4 for the endothermic side)
P	total pressure, Pa
P_i	partial pressure of component i, Pa
Q	total volumetric flow rate, $m^3.s^{-1}$
Q_0	constant in hydrogen permeation rate model, $mol.m^{-1}.s^{-1}.kPa^{-0.5}$
r_{CO}	rate of CO reaction, $mol.gr^{-1}.hr^{-1}$
r_{CO2}	rate of CO_2 reaction, $mol.gr^{-1}.hr^{-1}$
r_{DME}	rate of DME reaction, $mol.gr^{-1}.hr^{-1}$
r_{MeOH}	rate of methanol dehydrogenation reaction, $mol.gr^{-1}.hr^{-1}$
R	universal gas constant, $J.mol^{-1}.K^{-1}$
R_p	particle radius, m
T	temperature, K
u	superficial velocity of the fluid phase, $m.s^{-1}$
U_{1-2}	overall heat transfer coefficient between exothermic and endothermic sides, $W.m^{-2}.K^{-1}$
U_{2-3}	overall heat transfer coefficient between endothermic and permeation sides, $W.m^{-2}.K^{-1}$
X_{MeOH}	methanol conversion, dimensionless
X_{CO}	CO conversion, dimensionless
X_{H2}	H_2 conversion, dimensionless
X_{CO2}	CO_2 conversion, dimensionless
Y_{H2}	H_2 yield, dimensionless
y_i	mole fraction of component i
Y_{H2}	hydrogen recovery yield
z	axial reactor coordinate, m

GREEK LETTERS

ε	porosity (void fraction) of the catalytic bed
μ	viscosity of the fluid phase, $kg.m^{-1}.s^{-1}$(Pa.s)
ϕ_s	sphericity factor of the catalyst particles
ρ	density of the fluid phase, $kg.m^{-3}$
ρ_B	density of catalytic bed (ρB= ρ(1- ε)), $kg.m^{-3}$
η	catalyst effectiveness factor
β	β=0 for exothermic side and β=1 for endothermic side
φ	φ=1 for hydrogen and φ=0 for argon
δ_{H2}	membrane thickness, m

SUPERSCRIPTS

i	chemical species
j	reactor side (j=1 for exothermic side, j=2 for endothermic side, j=3 for permeation side)

SUBSCRIPTS

g	in bulk gas phase

APPENDIX A

Table 1: Peng-Robinson Equation of State (PR EOS) and Critical Properties of the Components

$$P = \frac{RT}{v-b} - \frac{a_c\alpha}{v(v+b)+b(v-b)} \quad (A1)$$

$$a_c = 0.457235\frac{R^2T_c^2}{P_c} \quad (A2)$$

$$b = 0.077796\frac{RT_c}{P_c} \quad (A3)$$

$$m = 0.37464 + 1.5422\omega - 0.26992\omega^2 \quad (A4)$$

$$\alpha = \left[1 + m\left(1 - \sqrt{T_r}\right)\right]^2 \quad (A5)$$

$$(a_c\alpha)_m = \sum_{i=1}^{NC}\sum_{j=1}^{NC} y_i y_j \sqrt{a_i a_j \alpha_i \alpha_j} \quad (A6)$$

$$b_m = \sum_{i=1}^{NC} y_i b_i \quad (A7)$$

$$A = \frac{(a_c\alpha)_m P}{(RT)^2} \quad (A8)$$

$$A = \frac{P(a_c\alpha)_m}{(RT)^2} \quad \text{(A9)}$$

$$B = \frac{Pb_m}{RT} \quad \text{(A10)}$$

$$Z^3 + (B-1)Z^2 + (A - 2B - 3B^2)Z - (AB - B^2 - B^3) = 0 \quad \text{(A11)}$$

$$\ln\frac{f_i}{y_i P} = \frac{b_i}{b_m}(Z-1) - \ln(Z-B) - \frac{A}{2\sqrt{2}B}\left[\frac{2\sum x_j\sqrt{a_i a_j \alpha_i \alpha_j}}{(a_c\alpha)_m} - \frac{b_i}{b_m}\right]\ln\left[\frac{Z + (1+\sqrt{2})B}{Z + (1-\sqrt{2})B}\right] \quad \text{(A12)}$$

Table A1: Critical Properties of Components

Component	T_c [K]	P_c [bar]	ω
MeOH	512.64	80.97	0.565
DME	400.10	54.00	0.274
H_2O	647.13	220.64	.345
MF	487.20	60.00	0.257
H_2	33.18	12.97	-0.216
CO	132.92	34.99	0.066
CO_2	304.19	73.82	0.228
CH_4	190.56	45.99	0.012
N_2	126.1	33.94	0.040
Ar	33.25	48.98	0

APPENDIX B

Table B1: Correlation of Specific Heat Capacity of the Components and Mixtures [82]

Heat Capacity ($J.kmol^{-1}.K^{-1}$)	$C_p = C_1 + C_2\left[\frac{C_3/T}{\sinh(C_3/T)}\right]^2 + C_4\left[\frac{C_5/T}{\cosh(C_5/T)}\right]^2$					(B1)
Component	**$C_1\times10^{-5}$**	**$C_2\times10^{-5}$**	**$C_3\times10^{-3}$**	**$C_4\times10^{-5}$**	**C_5**	
MeOH	0.3925	0.879	1.9165	0.5365	896.7	
DME	0.5148	1.442	1.6034	0.7747	725.4	
H_2O	0.3336	0.2679	2.6105	0.089	1169	
MF	0.506	1.219	1.637	0.894	743	
H_2	0.2762	0.0956	2.466	0.0376	567.6	
CO	0.2911	0.0877	3.0951	0.0846	1538.2	
CO_2	0.2937	0.3454	1.428	0.264	588.2	
CH_4	0.3333	0.7993	2.0869	0.416	991.96	
N_2	0.2911	0.0861	1.7016	0.001	909.79	
Ar	0.2079	-	-	-	-	
Mixture	$C_{p,mix} = \sum_{i=1}^{NC} y_i C_{p,i}$					(B2)

Table B2: Correlation of Viscosity of the Components and Mixtures [83, 84]

Viscosity (Pa.s)	$\mu = exp\left(A + \frac{B}{T} + C\log T + DT^E\right)$						(B3)
Component	**A**	**B**	**C**	**D**	**E**	**MW ($gr.mol^{-1}$)**	
MeOH	-7.288	1065.3	-0.6657	0	0	32	

DME	-10.62	448.99	8.396×10^{-5}	0	0	46	
H_2O	-51.964	3670.6	5.7331	-5.349×10^{-29}	10	18	
Viscosity (Pa.s)	$\mu = \frac{AT^B}{1 + CT^{-1} + DT^E}$						(B4)
	A×10^6	**B**	**C**	**D**	**E**	**MW (gr.mol^{-1})**	
MF	1.6672	0.47948	516.01	0	0	60.05	
H_2	1.0009	0.47949	290.01	0	0	2	
Ar	4.71912	0.40949	390.01	0	0	39.95	
CO	2.59835	0.48028	517.84	0	0	28	
CO_2	2.34271	0.480291	550.72	0	0	44	
N_2	4.63771	0.39118	533.73	0	0	28	
Mixture	$\mu_{mix} = \frac{\sum_{i=1}^{NC} y_i \mu_i MW_i^{0.5}}{\sum_{i=1}^{NC} y_i MW_i^{0.5}}$						(B5)

Table B3: Correlation of Thermal Conductivity of the Components and Mixtures [84, 85]

Thermal Conductivity (J/m.K.sec)	$k_{th} = A + BT + CT^2 + DT^3$				(B6)
Component	**A×10^2**	**B×10^5**	**C×10^7**	**D×10^{11}**	
MeOH	-1.8683	8.7959	0.82324	-2.8949	
DME	-0.83897	5.8126	1.1178	-4.0608	
H_2O	0.56199	1.5699	1.0106	-2.4282	
MF	0.085	0.60228	1.2439	0	
H_2	1.0979	66.411	-3.4378	9.7283	
Ar	-0.30142	6.8128	-0.3182	0.6854	
CO	0.099186	9.4020	-0.40761	1.3751	
CO_2	-1.2	10.208	-0.22403	0	
CH_4	0.53767	5.1555	1.6655	-5.7168	
N_2	-0.02268	10.275	-0.60151	2.2332	
Mixture	$k_{th,mix} = \sum_{i=1}^{NC} y_i k_i$				(B7)

Table B4: Heat Transfer Coefficient of Reaction Side, Membrane Side and Overall Heat Transfer Coefficient

Reaction sides [86]
$$\frac{h}{\rho u C_p}\left(\frac{C_p \mu}{k_{th}}\right)^{2/3} = \frac{0.4548}{\varepsilon}\left(\frac{\rho u d_p}{\mu}\right)^{-0.407} \quad \text{(B8)}$$

Membrane sides [87]
$$h = 0.0214\frac{k_{th}}{D}Pr^{0.4}(Re_D^{0.8} - 100) \quad \text{(B9)}$$

Overall coefficient
$$\frac{1}{U} = \frac{1}{h_i} + \frac{A_i \ln(D_o/D_i)}{2\pi z k_w} + \frac{A_i}{A_o}\frac{1}{h_o} \quad \text{(B10)}$$

It should be mentioned that in equation B8, C_p is used in mass units (J.kg^{-1}.K^{-1}) therefore the *Cp* calculated from equation B2 must be multiplied by average molecular weight.

REFERENCES

[1] Ross M. Energy Consumption by Industry. Ann Rev Energy 1981; 6: 379-416. http://dx.doi.org/10.1146/annurev.eg.06.110181.002115

[2] Axelsson H, Asblad A, Berntsson T. A new methodology for greenhouse gas reduction in industry through improved heat exchanging and/or integration of combined heat and power, Applied Thermal Engineering 1999; 19: 707-31. http://dx.doi.org/10.1016/S1359-4311(98)00084-2

[3] Ebrahim M, Kawari A. Pinch technology: an efficient tool for chemical-plant energy and capital-cost saving, Applied Energy 2000; 65: 45-9. http://dx.doi.org/10.1016/S0306-2619(99)00057-4

[4] Jegla Z, Stehlı'k P, Kohoutek J. Plant energy saving through efficient retrofit of furnaces, Applied Thermal Engineering 2000; 20: 1545-60. http://dx.doi.org/10.1016/S1359-4311(00)00031-4

[5] Friedler F. Process integration, modeling and optimization for energy saving and pollution reduction. Appl Therm Eng 2010; 30: 2270-80. http://dx.doi.org/10.1016/j.applthermaleng.2010.04.030

[6] Smith R. State of the art in process integration. Appl Therm Eng. 2000; 20: 1337-45. http://dx.doi.org/10.1016/S1359-4311(00)00010-7

[7] Rossiter AP. Succeeding in process integration. In: Process industries expo user conference. 2003.

[8] Rahimpour MR, Dehnavi MR, Allahgholipour F, Iranshahi D, Jokar SM. Assessment and comparison of different catalytic coupling exothermic and endothermic reactions: A review, Applied Energy 2012; 99: 496-512. http://dx.doi.org/10.1016/j.apenergy.2012.04.003

[9] Rahimpour MR, Bahmanpour AM. Optimization of hydrogen production via coupling of the Fischer–Tropsch synthesis reaction and dehydrogenation of cyclohexane in GTL technology. Appl Energy 2011; 88: 2027-36. http://dx.doi.org/10.1016/j.apenergy.2010.12.065

[10] Rahimpour MR, Khademi MH, Bahmanpour AM. A comparison of conventional and optimized thermally coupled reactors for Fischer–Tropsch synthesis in GTL technology Chem Eng Sci 2010; 65: 6206-14. http://dx.doi.org/10.1016/j.ces.2010.09.002

[11] Rahimpour MR, Mirvakili A, Paymooni K. Simultaneous hydrogen production and utilization via coupling of Fischer–Tropsch synthesis and decalin dehydrogenation reactions in GTL technology. Int J Hydrogen Energy 2010; 36: 2992-3006. http://dx.doi.org/10.1016/j.ijhydene.2010.11.099

[12] Rahimpour MR, Mirvakili A, Paymooni K. Differential evolution (DE) strategy for optimization of hydrogen production and utilization in a thermally coupled membrane reactor for decalin dehydrogenation and Fischer–Tropsch synthesis in GTL technology. Int J Hydrogen Energy 2010; 36: 4917-33. http://dx.doi.org/10.1016/j.ijhydene.2011.01.061

[13] Rahimpour MR. Enhancement of hydrogen production in a novel fluidized bed membrane reactor for naphtha reforming. Int J Hydrogen Energy 2009; 34: 2235-51. http://dx.doi.org/10.1016/j.ijhydene.2008.10.098

[14] Rahimpour MR, Vakili R, Pourazadi E, Iranshahi D, Paymooni K. A novel integrated, thermally coupled fluidized bed configuration for catalytic naphtha reforming to enhance aromatic and hydrogen productions in refineries. Int J Hydrogen Energy 2011; 36: 2979-91. http://dx.doi.org/10.1016/j.ijhydene.2010.11.112

[15] Iranshahi D, Pourazadi E, Bahmanpour AM, Rahimpour MR. A comparison of two different flow types on performance of a thermally coupled recuperative reactor containing naphtha reforming process and hydrogenation of nitrobenzene. Int J Hydrogen Energy 2011; 36: 3483-95. http://dx.doi.org/10.1016/j.ijhydene.2010.12.033

[16] Iranshahi D, Bahmanpour AM, Pourazadi E, Rahimpour MR. Mathematical modeling of a multi-stage naphtha reforming processusing novel thermally coupled recuperative reactors to enhance aromatic production. Int J Hydrogen Energy 2010; 35: 10984-93. http://dx.doi.org/10.1016/j.ijhydene.2010.07.077

[17] Vakili R, Pourazadi E, Setoodeh P, Eslamloueyan R, Rahimpour MR. Direct dimethyl ether (DME) synthesis through a thermally coupled heat exchanger reactor. Appl Energy 2011; 88: 1211-23. http://dx.doi.org/10.1016/j.apenergy.2010.10.023

[18] Bayat M, Rahimpour MR. Production of ultrapure hydrogen via utilizing fluidization concept from coupling of methanol and benzene synthesis in a hydrogen perm-selective membrane reactor. Int J Hydrogen Energy 2011; 36: 6616-27. http://dx.doi.org/10.1016/j.ijhydene.2011.02.095

[19] Khademi MH, Rahimpour MR, Jahanmiri A. Differential evolution (DE) strategy for optimization of hydrogen production, cyclohexane dehydrogenation and methanol synthesis in a hydrogen-permselective membrane thermally coupled reactor. Int J Hydrogen Energy 2010; 35: 1936-50. http://dx.doi.org/10.1016/j.ijhydene.2009.12.080

[20] Khademi MH, Setoodeh P, Rahimpour MR. Jahanmiri A. Optimization of methanol synthesis and cyclohexane dehydrogenation in a thermally coupled reactor using differential evolution (DE) method. Int J Hydrogen Energy 2009; 34: 6930-44. http://dx.doi.org/10.1016/j.ijhydene.2009.06.018

[21] Arab Aboosadi Z, Rahimpour MR, Jahanmiri A. A novel integrated thermally coupled configuration for methane-steam reforming and hydrogenation of nitrobenzene to aniline. Int J Hydrogen Energy 2011; 36: 2960-8. http://dx.doi.org/10.1016/j.ijhydene.2010.12.005

[22] Vakili R, Setoodeh P, Pourazadi E, Iranshahi D, Rahimpour MR. Utilizing differential evolution (DE) technique to optimize operating conditions of an integrated thermally coupled direct DME synthesis reactor. Chem Eng J 2011; 168: 321-32. http://dx.doi.org/10.1016/j.cej.2011.01.032

[23] Rahimpour MR, Vakili R, Pourazadi E, Bahmanpour AM. Iranshahi D. Enhancement of hydrogen production via coupling of MCH dehydrogenation reaction and methanol synthesis process by using thermally coupled heat exchanger reactor. Int J Hydrogen Energy 2011; 36: 3371-83. http://dx.doi.org/10.1016/j.ijhydene.2010.12.073

[24] Rahimpour MR, Pourazadi E. A comparison of hydrogen and methanol production in a thermally coupled membrane reactor for co current and counter current flows. Int J Energy Res. 2010; 35: 863-82. http://dx.doi.org/10.1002/er.1744

[25] Rahimpour MR, Rahmani F, Bayat M, Pourazadi E. Enhancement of simultaneous hydrogen production and methanol synthesis in thermally coupled double-membrane reactor. Int J Hydrogen Energy 2010; 36: 284-98. http://dx.doi.org/10.1016/j.ijhydene.2010.09.074

[26] Bayat M, Rahimpour MR. Simultaneous utilization of two different membranes for intensification of ultrapure hydrogen production from recuperative coupling auto thermal multi tubular reactor. Int J Hydrogen Energy 2011; 36: 7310-25. http://dx.doi.org/10.1016/j.ijhydene.2011.02.051

[27] Rahimpour MR, Mirvakili A, Paymooni K. Hydrogen as an energy carrier: a comparative study between decalin and cyclohexane in thermally coupled membrane reactors in gas-to-liquid technology. Int J Hydrogen Energy 2010; 36: 6970-84. http://dx.doi.org/10.1016/j.ijhydene.2011.03.007

[28] Rahimpour MR. Membrane reactors for biodiesel production and processing.Membrane Reactors for Energy Applications and Basic Chemical Production. http: //dx.doi.org/10.1016/B978-1-78242-223-5.00010-8

[29] Rahimpour MR. Buteneoligomerization, phenol synthesis from benzene, butane partial oxidation, and other reactions carried out in membrane reactors. Membrane Reactors for Energy Applications and Basic Chemical Production. http: //dx.doi.org/10.1016/B978-1-78242-223-5.00021-2

[30] Jana AK. Heat integrated distillation operation. Appl. Energy 2010; 87: 1477-94. http://dx.doi.org/10.1016/j.apenergy.2009.10.014

[31] Rohde MP, Schaub G, Khajavi S, Janse JC, Kapteijn F. Fischere Tropsch synthesis with in situ H2O removal - directions of membrane development. Microp Mesop Mater

2008; 115: 123-36.
http://dx.doi.org/10.1016/j.micromeso.2007.10.052

[32] Fernandes FAN, Soares AB Jr. Methane steam reforming modeling in a palladium membrane reactor. Fuel 2006; 85: 569-73.
http://dx.doi.org/10.1016/j.fuel.2005.08.002

[33] Khajavi S, Jansen JC, Kapteijn F. Application of a sodalite membrane reactor in esterification coupling reaction and separation. Catal. Today 2010; 156: 132-9.
http://dx.doi.org/10.1016/j.cattod.2010.02.042

[34] Mirvakili A, Paymooni K. Rahimpour MR. A novel water perm-selective membrane dual-type reactor concept for Fischere Tropsch synthesis of GTL (gas to liquid) technology Energy 2011; 36: 1223-35.
http://dx.doi.org/10.1016/j.energy.2010.11.023

[35] Nigam PS, Singh A. Production of liquid biofuels from renewable resources. Prog En Combust Sci 2011; 37: 52-68.
http://dx.doi.org/10.1016/j.pecs.2010.01.003

[36] Zhang L, Wang J, Wu P, Hou Z, Fei X. Synthesis of dimethyl ether via methanol dehydration over combined Al2O3-HZSM-5 solid-acids. Chin. J Catal 2010; 31: 987-92.
http://dx.doi.org/10.1016/S1872-2067(10)60098-8

[37] Azizi Z, Rezaeimanesh M, Tohidian T, Rahimpour MR. Dimethyl ether: A review of technologies and production challenges. Chem Eng and Proc: Process Int 2014; 82: 150-72.
http://dx.doi.org/10.1016/j.cep.2014.06.007

[38] Raoof F, Taghizadeh M, Eliassi A, Yaripour F. Effects of temperature and feed composition on catalytic dehydration of methanol to dimethyl ether over-alumina. Fuel 2008; 87: 2967-71.
http://dx.doi.org/10.1016/j.fuel.2008.03.025

[39] Chen WH, Lin BJ, Lee HM Huang MH. One-step synthesis of dimethyl ether from the gas mixture containing CO2 with high space velocity. Appl Energy 2012; 98: 92-101.
http://dx.doi.org/10.1016/j.apenergy.2012.02.082

[40] Ladera R, Finocchio E, Rojas S, Fierro JLG, Ojeda M. Supported niobium catalysts for methanol dehydration to dimethyl ether: FTIR studies of acid properties. Catal Today 2012; 192: 136-43.
http://dx.doi.org/10.1016/j.cattod.2012.01.025

[41] Tokay KC, Dogu T, Dogu G. Dimethyl ether synthesis over alumina based catalysts. Chem Eng J 2012; 184: 275-85.
http://dx.doi.org/10.1016/j.cej.2011.12.034

[42] Hayer F, Bakhtiary Davijany H, Myrstad R, Holmen A, Pfeifer P, Venvik HJ. Characteristics of integrated micro packed bed reactor-heat exchanger configurations in the direct synthesis of dimethyl ether. Chem Eng Process 2013; 70: 77-85.
http://dx.doi.org/10.1016/j.cep.2013.03.021

[43] Faungnawakij K, Tanaka Y, Shimoda N, Fukunaga T, Kikuchi R, Eguchi K. Hydrogen production from dimethyl ether steam reforming over composite catalysts of copper ferrite spinel and alumina. Appl Catal B: Environ 2007; 74: 144-51.
http://dx.doi.org/10.1016/j.apcatb.2007.02.010

[44] Ren E, Wang JF, Li HS. Direct mass production technique of dimethyl ether from synthesis gas in a circulating slurry bed reactor. Stud Surf Sci Catal 2006; 159: 489-92.
http://dx.doi.org/10.1016/S0167-2991(06)81640-X

[45] Gadek M, Kubica R, Jedrysik E. Production of methanol and dimethyl ether from biomass derived syngas: a comparison of the different synthesis path ways by means of flowsheet simulation. in: The 23rd European Symposium on Computer Aided Process Engineering (ESCAPE 23) 2013.
http://dx.doi.org/10.1016/B978-0-444-63234-0.50010-5

[46] Hu Y, Nie Z, Fang D. Simulation and model design of pipe-shell reactor for the direct synthesis of dimethyl ether from syngas. Journal of Natural Gas Chemistry 2008; 17: 195-200.
http://dx.doi.org/10.1016/S1003-9953(08)60051-1

[47] Lu WZ, Teng LH, Xiao WD. Simulation and experiment study of Dimethyl ether synthesis from syngas in a fluidized-bed reactor. Chem Eng Sci 2440; 59: 5455-64.
http://dx.doi.org/10.1016/j.ces.2004.07.031

[48] Nie Z, Liu H, Ying W, Fang D. Intrinsic kinetics of dimethyl ether synthesis from syngas. Journal of Natural Gas Chemistry 2005; 14: 22-8.

[49] You Q, Liu Z, Li W, Zhou X. Synthesis of dimethyl ether from methane mediated by HBr, J Nat Gas Chem 2009; 18: 3006-3011.

http://dx.doi.org/10.1016/S1003-9953(08)60122-X

[50] Wang Y, Wang WL, Chen YX, Zheng JJ, Li RF. Synthesis of dimethyl ether from syngas using a hierarchically porous composite zeolite as the methanol dehydration catalyst, J. Fuel Chem. Technol. 2013; 14: 873-82.
http://dx.doi.org/10.1016/S1872-5813(13)60037-7

[51] Lee JS, Kim JC, Kin YG. Methyl Formate as a new building block in C1 chemistry. Applied Catalysis 1990; 57: 1-30.
http://dx.doi.org/10.1016/S0166-9834(00)80720-4

[52] Jenner G. Homogeneous catalytic reactions involving methyl formate. Applied Catalysis A: General 1995; 12: 25-44.
http://dx.doi.org/10.1016/0926-860X(95)85008-2

[53] Keim W. Catalysis in C1 Chemistry. Netherlands: Springer; 1983.
http://dx.doi.org/10.1007/978-94-009-7040-3

[54] Wender I. Chemicals from methanol. Catal Rev 1984; 26: 303-21.
http://dx.doi.org/10.1080/01614948408064715

[55] Calkins WH, Chemicals from methanol Catal Rev 1984; 26: 347-58.
http://dx.doi.org/10.1080/01614948408064717

[56] Jiang R, Guo W, Li M, Zhu H, Zhao L, Lu X, Shan H. Methanol dehydrogenation on Rh(1 1 1): A density functional and microkinetic modeling study. Journal of Molecular Catalysis A: Chemical 2011; 344: 99-110.
http://dx.doi.org/10.1016/j.molcata.2011.05.007

[57] Couteau W, Ramioulle J. US Patent US4216339.

[58] Wang W, Wang Y. Thermodynamic analysis of hydrogen production via partial oxidation of ethanol. Int J Hydrogen Energy 2008; 33: 5035-44.
http://dx.doi.org/10.1016/j.ijhydene.2008.07.086

[59] Rahimpour MR, M. Farniaei M, Abbasi M, Javanmardi J, Kabiri S. Comparative study on simultaneous production of methanol, hydrogen, and DME using a novel integrated thermally double-coupled reactor. Energy Fuels 2013; 27: 1982-93.
http://dx.doi.org/10.1021/ef301683j

[60] Brown LF. A comparative study of fuels for on-board hydrogen production for fuel-cell-powered automobiles. Int. J. Hydrogen Energy 2001; 26: 381-97.
http://dx.doi.org/10.1016/S0360-3199(00)00092-6

[61] Itoh N, Watanabe S, Kawasoe K, Sato T, Tsuji TA. A membrane reactor for hydrogen storage and transport system using cyclohexane-methylcyclohexane mixtures. Desalination 2008; 234: 261-9.
http://dx.doi.org/10.1016/j.desal.2007.09.093

[62] Momirlan M, Veziroglu T. Current status of hydrogen energy. Renewable and Sustainable Energy Reviews 2002; 6: 141-79.
http://dx.doi.org/10.1016/S1364-0321(02)00004-7

[63] Palma V, Vaiano V, Barba D, Colozzi M, Palo E, Barbato L, Cortese S. H2 production by thermal decomposition of H2S in the presence of oxygen. Int J Hydrogen Energy 2015; 40: 106-13.
http://dx.doi.org/10.1016/j.ijhydene.2014.11.022

[64] Rahimpour MR, Pourazadi E. A comparison of hydrogen and methanol production in a thermally coupled membrane reactor for co-current and counter-current flows. Int J Energy

Res. 2011; 35: 863-82.
http://dx.doi.org/10.1002/er.1744

[65] Farniaei M, Abbasi M, Rasoolzadeh A, Rahimpour MR, Enhancement of methanol, DME and hydrogen production via employing hydrogen perm-selective membranes in a novel integrated thermally double-coupled two-membrane reactor. J Nat Gas Sci Eng 2013; 14: 158-73.
http://dx.doi.org/10.1016/j.jngse.2013.06.010

[66] Vakili R, Rahimpour MR, Eslamloueyan R. Incorporating differential evolution (DE) optimization strategy to boost hydrogen and DME production rate through a membrane assisted single-step DME heat exchanger reactor. J. of Nat. Gas Sci and Eng 2012; 9: 28-38.
http://dx.doi.org/10.1016/j.jngse.2012.05.006

[67] Vakili R, Rahmanifard H, Maroufi P, Eslamloueyan R, Rahimpour MR. The effect of flow type patterns in a novel thermally coupled reactor for simultaneous direct dimethyl ether (DME) and hydrogen production. Int J Hydrogen Energy 2011; 36: 4354-65.
http://dx.doi.org/10.1016/j.ijhydene.2010.12.135

[68] Farsi M, Khademi MH, Jahanmiri A, Rahimpour MR. Novel recuperative configuration for coupling of methanol dehydration to dimethyl ether with cyclohexane dehydrogenation to benzene. Ind Eng Chem Res 2010; 49: 4633-43.
http://dx.doi.org/10.1021/ie1000086

[69] Khademi MH Farsi M, Rahimpour MR, Jahanmiri A. DME synthesis and cyclohexane dehydrogenation reaction in an optimized thermally coupled reactor. Chem Eng and Proc 2011; 50: 113-23.
http://dx.doi.org/10.1016/j.cep.2010.12.004

[70] Farsi M, Khademi MH, Jahanmiri A, Rahimpour MR. Optimal conditions for hydrogen production from coupling of dimethyl ether and benzene synthesis. Int. J Hydrogen Energy 2010; 36: 299-310.
http://dx.doi.org/10.1016/j.ijhydene.2010.10.049

[71] Goosheneshin A, Maleki R, Iranshahi D, Rahimpour MR, Jahanmiri A. Simultaneous production and utilization of methanol for methyl formate synthesis in a looped heat exchanger reactor configuration. Journal of Natural Gas Chemistry 2010; 21: 661-72.
http://dx.doi.org/10.1016/S1003-9953(11)60417-9

[72] Bakhtyari A, Mohammadi M, Rahimpour MR. Simultaneous production of dimethyl ether (DME), methyl formate (MF) and hydrogen from methanol in an integrated thermally coupled membrane reactor, J of Nat Gas Sci and Eng 2015; 26: 595-607.
http://dx.doi.org/10.1016/j.jngse.2015.06.052

[73] Huang X, Cant NW, Wainwright MS, Ma L. The dehydrogenation of methanol to methyl formate Part I: Kinetic studies using copper-based catalysts. Chemical Engineering and Processing 2005; 44: 393-402.

[74] Shu J, Grandjean BPA, Neste AV, Kaliaguine S. Catalytic palladium-based membrane reactors: a review. Canadian Journal of Chemical Engineering 1991; 69: 1036-60.
http://dx.doi.org/10.1002/cjce.5450690503

[75] Uemiya S, Matsuda T, Kikuchi E. Hydrogen permeable palladium-alloy membrane supported on porous ceramics. Journal of Membrane Science 1991; 56: 315-25.
http://dx.doi.org/10.1016/S0376-7388(00)83041-0

[76] McLeod LS. Hydrogen permeation through micro fabricated palladium-silver alloy membranes. PhD Thesis. Georgia Institute of Technology, December 2008.

[77] Barbieri G, Di Maio FP. Simulation of the methane steam re-forming process in a catalytic Pd-membrane reactor. Ind Eng Chem Res 1997; 36: 2121-7.
http://dx.doi.org/10.1021/ie9601615

[78] Rahnama H, Farniaei M, Abbasi M, Rahimpour MR. Modeling of synthesis gas and hydrogen production in a thermally coupling of steam and tri-reforming of methane with membranes. Journal of Industrial and Engineering Chemistry 2014; 20: 1779-92.
http://dx.doi.org/10.1016/j.jiec.2013.08.032

[79] Schwefel HP. Numerical Optimization of Computer Models. New York: John Wiley & Sons; 1981.

[80] Goldberg DE. Genetic algorithms in search, optimization, and machine learning, Addison-Wesley, Reading, MA, 1989.

[81] Rahimpour MR, Elekaei Behjati H. Dynamic optimization of membrane dual-type methanol reactor in the presence of catalyst deactivation using genetic algorithm, Fuel Processing Technology 2009; 90: 279-91.
http://dx.doi.org/10.1016/j.fuproc.2008.09.008

[82] Perry RH, Green DW, Perry's chemical engineering handbook. New York: McGraw Hill; 1999.

[83] Viswanath DS, Ghosh TK, Prasad DHL, Dutt NVK, Rani KY. Viscosity of Liquids: Theory, Estimation, Experiment, and Data. Netherlands: Springer; 2007.

[84] Yaws CL. Transport properties of chemicals and hydrocarbons: viscosity, thermal conductivity, and diffusivity of Clto Cl00 organics and Ac to Zr inorganic. William Andrew Inc.; 2009.

[85] Yaws CL, Handbook of Thermal Conductivity. Gulf Publishing Company; 1995.

[86] Dwivedi PN, Upadhyay SN. Particle-Fluid Mass Transfer in Fixed and Fluidized Beds. Ind Eng Chem Process Des. Dev 1977; 16: 157-65.
http://dx.doi.org/10.1021/i260062a001

[87] Holman JP. Heat transfer. New York: McGraw-Hill; 1989.

Received on 29-10-2015 Accepted on 15-07-2016 Published on 30-11-2016

http://dx.doi.org/10.15379/2410-1869.2016.03.02.01